Structural Defects Induced in ETS-10 by Postsynthesis Treatment with H_2O_2 Solution

Claudiu C. Pavel,[†] So-Hyun Park,[†,‡] Axel Dreier,[†] Bernd Tesche,[†] and Wolfgang Schmidt*[,†]

Max-Planck-Institut für Kohlenforschung, Kaiser-Wilhelm-Platz 1, 45470 Mülheim an der Ruhr, Germany, and Department Geo- und Environmental Science, Section Crystallography, Ludwig-Maximilians-Universität München, Theresienstrass 41, 80333 München, Germany

Received October 12, 2005. Revised Manuscript Received April 28, 2006

The presence of structural defects in ETS-10 titanosilicate plays an important role in its adsorption capacity and catalytic activity, e.g., in photocatalysis of organic molecules. In the present work, we used postsynthesis treatments with hydrogen peroxide to introduce different levels of defects in the ETS-10 structure. The number of defects induced was dependent on the concentration of H_2O_2 and exposition time. These treatments led to a partial removal of Ti atoms, resulting in the interruption of titania chains and the consequent formation of larger micropores (supermicropores) without substantial degradation of crystallinity. High-resolution sorption experiments indicate that the micropore volume was slightly increased after H_2O_2 treatment, and a bimodal pore size distribution was observed for the modified ETS-10 samples. The presence of supermicropores in the structure was directly visualized by transmission electron microscopy. The interruption of Ti−O−Ti chains and the formation of new accessible Ti centers was indicated by spectroscopic techniques such as Raman, DRIFT, and DR UV−vis spectroscopy.

Introduction

Engelhard titanosilicate (ETS-10), a microporous crystalline material discovered by Kuznicki in 1989,[1] is a large-pore zeotype (pore opening of about 0.8 nm) with the composition $M_2TiSi_5O_{13}\cdot nH_2O$ (M = Na, K).[2,3] In the ETS-10 structure, chains of TiO_6 octahedra are linked to SiO_4 tetrahedra to form $[TiSi_4O_{13}]$ columns that are packed into layers parallel to the (001) plane, with the columns in adjacent layers perpendicular to each other.[4] The layers are interconnected by other SiO_4 tetrahedra, forming a three-dimensional structure. This framework contains three orthogonal sets of channels along the *a*, *b*, and *c* axes, defined by rings containing 12 silicon atoms (12-MR). The channels are straight in the [100] and [010] directions and curved along [001]. A considerable degree of stacking disorder occurs in ETS-10 along its (001) plane. The real structure can be described as an intergrowth of two hypothetical ordered polymorphs, each formed by a particular stacking arrangement:[2,3] the tetragonal polymorph A (space group $P4_1$ or $P4_3$), characterized by an ABAB stacking sequence of the layers, and the monoclinic polymorph B (space group $C2/c$), characterized by an ABCD sequence, as shown in Figure 1.

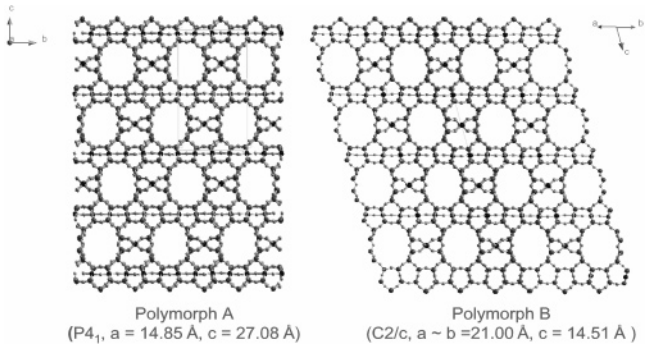

Figure 1. Hypothetical polymorphs of ETS-10 looking along the straight channels.

Recently, Aspin et al.[5] have observed a vertical AAA stacking sequence in electron micrographs of ETS-10, which is not characteristic for this material. The authors hypothesized the presence of a third polymorph C, called CMM-5, intergrowing within ETS-10. Titanosilicate ETS-10 has attracted attention in adsorption, ion exchange, and shape-selective catalysis for a number of reasons: (i) it has a three-dimensional pore system that allows good diffusional access; (ii) it has a high cation-exchange capacity because exchangeable Na^+ and K^+ cations balance the two negative changes generated by the presence of $[TiO_6]^{2-}$ octahedra; (iii) it possesses electronically isolated titanate (O−Ti−O−Ti) chains that may act as quantum wires with modified optoelectronic properties; and (iv) it contains a high concentration of defects as the result of the fusion of adjacent

* To whom correspondence should be addressed. E-mail: wolfgang.schmidt@mpi-muelheim.mpg.de. Tel: 49-208-3062309. Fax: 49-208-3062995.
† Max-Planck-Institut für Kohlenforschung.
‡ Ludwig-Maximilians-Universität München.

(1) Kuznicki, S. M. U.S. Patent 4 853 202, 1989.
(2) Anderson, M. W.; Terasaki, O.; Ohsuna, T.; Philippou, A.; MacKay, S. P.; Ferreira, A.; Rocha, J.; Lidin, S. *Nature* **1994**, *367*, 347.
(3) Anderson, M. W.; Terasaki, O.; Ohsuna, T.; Malley, P. J. O.; Philippou, A.; MacKay, S. P.; Ferreira, A.; Rocha, J.; Lidin, S. *Philos. Mag. B* **1995**, *71*, 813.
(4) Wang, X.; Jacobson, A. J. *Chem. Commun.* **1999**, 973.
(5) Aspin, P.; Hanif, N.; Anderson, M. W.; Cundy, C. S. In *Recent Advances in the Science and Technology of Zeolites and Related Materials*; Proceedings of the 14th International Zeolite Conference, Cape Town, South Africa, April 25-30, 2004; van Steen, E., Callanan, L. H., Claeysp, M., Eds; Elsevier: New York, 2004; 1303.

10.1021/cm052261j CCC: $33.50
Published on Web 07/06/2006

pores. These larger pores allow for easier access to the internal void space and furthermore provide active sites for catalysis.[6,7] Recently, ETS-10 became particularly interesting for photocatalytic applications. Examples are the oxidation of organic alcohols by ETS-10 within the pores of zeolitic supports;[8] the shape-selectivity effects in oxidative photodegradation of organic molecules (phenols);[9] and the photocatalytic decomposition of acetaldehyde over ETS-10 and transition metals incorporated in ETS-10.[10] Howe and Krisnandi concluded that the photocatalytic activity of ETS-10 is strongly influenced by stacking fault defects and ion-exchange-induced external defects present in the structure.[11,12] The effect of the concentration of stacking faults obtained by different preparation methods of ETS-10 on the spectroscopic properties was investigated by Southon and Howe.[13] They showed that even well-crystalline ETS-10 samples exhibit significant variations in short-range order.

For catalytic applications, a major challenge is finding ways to manipulate the abundance and type (double pores, line defects, stacking faults) of defects in the ETS-10 structure. One possibility for introducing defects is to form them directly during the hydrothermal synthesis by varying synthesis parameters such as temperature, heating rate, or starting reagents or by adding structure-directing agents. Anderson et al.[14] assume that defects sites are caused by the existence of a high concentration of terrace nuclei on a growing surface, and in order to increase the number of defects, it seems important to increase the rate of terrace nucleation relative to the rate of growth of the terrace. However, the crystallization process is probably not well enough understood to permit the prediction of a specific concentration in this material. An alternative for creating defects in ETS-10 are postsynthesis treatments, but little detailed work has been performed in this direction. Koermer et al.[15] treated ETS-10 with citric acid; a certain fraction of Ti atoms was extracted from the titanosilicate framework, resulting in an increased Si:Ti ratio and the generation of active Ti species. The obtained titanosilicate was active in alkene epoxidation (5−10% conversion of the organic substrate). Recently, Llabrés i Xamena et al.[16] described postsynthesis modifications of ETS-10 via acid treatment with diluted HF solution, causing a partial dissolution of SiO_2 surrounding the Ti−O−Ti chains. With this treatment, the amount of accessible titanium centers for photodegradation of organic molecules was increased. Goa et al.[17] recently reported changes in the coordination environment of Ti atoms after treatments of ETS-10 with HCl, NH_4Cl, and citric acid. The authors found that these treatments led to a partial detitanation of ETS-10 and reported that the structure starts to collapse after removal of more than 5 mol % Ti. The thus-treated ETS-10 was found to be active in the epoxidation of cyclohexene using H_2O_2 as the oxidant.

Here, we report a simple method for generating new structural defects into ETS-10 by postsynthesis treatment with hydrogen peroxide solutions. Our aim was to investigate the effects of the partial leaching of titanium atoms from the framework on the formation of larger pores in the crystallites and new active Ti centers.

Experimental Section

Material Preparations. The hydrothermal synthesis of ETS-10 titanosilicate was performed from a gel with the molar composition 5.0 SiO_2:1.0 TiO_2:7.0 Na_2O: 0.75 K_2O: 150 H_2O, using Ludox AS-40 colloidal silica and $TiCl_3$ solution as the Si and Ti sources. In a typical preparation, 5.6 g of sodium hydroxide pellets (97+%, Aldrich) and 0.88 g of potassium fluoride spray-dried (99%, Aldrich) were dissolved in 12.47 g of deionized water and then mixed with 7.51 g of Ludox AS-40 colloidal silica (40 wt % suspension in water, Sigma-Aldrich) in a 100 mL polypropylene beaker. To this solution was added 15.42 g of a titanium (III) chloride solution (10 wt % in 20−30 wt % hydrochloric acid, Aldrich). Finally, 0.1 g of ETS-10 was added as crystallization seeds. The resulting gel was vigorously stirred for 10 min and then transferred into a 50 mL Teflon-lined stainless steel autoclave; it was finally allowed to react under static conditions at 463 K for 6 days. The resulting solid was recovered by filtration, washed with deionized water, and dried at 353 K overnight.

To induce defects and investigate the influence of H_2O_2 on the microporosity of ETS-10, we gently stirred 0.5 g of ETS-10 in 50 mL of an aqueous solution of hydrogen peroxide of different concentrations, ranging from 5 to 30 wt %, at room temperature for different times. In a second series, 0.5 g of ETS-10 was treated three times with fresh 10 wt % H_2O_2 solution for 20 min each time. The sample notation, treatment conditions, and quantity of Ti leached from the samples are listed in Table 1. After the H_2O_2 treatments, the crystalline phases were separated from the solution by centrifugation, washed well with deionized water, and dried at 353 K for 6 h. The bright yellow H_2O_2 solutions were analyzed quantitatively with an Eppendorf 1101M photometer with respect to their titanium content immediately after the separation of the solids.

Characterization of Materials. Aqueous solutions of Ti (IV) containing hydrogen peroxide have an intense orange color, which can be used for the quantitative analysis of the Ti content. The content of Ti in the H_2O_2 solutions separated after postsynthesis treatments was determined by photocolorimetric measurements of the peroxo complex $[Ti(O_2)OH_{aq})]^+$ formed under alkaline conditions at a wavelength of 405 nm. A titanium standard solution (991 μg ml^{-1}, Aldrich) was used to construct the calibration curve. The effect of H_2O_2 treatment on the crystallinity of the samples was investigated by powder X-ray diffraction on a Stoe STADI P transmission diffractometer using Cu Kα1 radiation. The porous properties of the ETS-10 samples were determined from nitrogen adsorption measurements at 77 K and argon adsorption measure-

(6) Rocha, J.; Anderson, M. W. *Eur. J. Inorg. Chem.* **2000**, 801.
(7) Anderson, M. W.; Agger, J. R.; Hanif, N.; Terasaki, O. *Microporous Mesoporous Mater.* **2001**, *48*, 1.
(8) Fox, M. A.; Doan, K. E.; Dulay, M. T. *Res. Chem. Intermed.* **1994**, *20*, 711.
(9) Calza, P.; Pazé, C.; Pelizzetti, E.; Zecchina, A. *Chem. Commun.* **2001**, 2130.
(10) Uma, S.; Rodrigues, S.; Martyanov, I. N.; Klabunde, K. J. *Microporous Mesoporous Mater.* **2004**, *67*, 181.
(11) Howe, R. F.; Krisnandi, Y. K. *Chem. Commun.* **2001**, 1588.
(12) Krisnaldi, Y. K.; Southon, P. D.; Adesina, A. A.; Howe, R. F. *Int. J. Photoenergy* **2003**, *5*, 131.
(13) Southon, P. D.; Howe, R. F. *Chem. Mater.* **2002**, *14*, 4209.
(14) Anderson, M. W.; Agger, J. R.; Hanif, N.; Terasaki, O.; Ohsuna, T. *Solid State Sci.* **2001**, *3*, 809.
(15) Koermer, G.; Thangaraj, A.; Kuznicki. S. *Stud. Surf. Sci. Catal.* **2001**, *135*, 1619.
(16) Llabrés i Xamena, F. X.; Calza, P.; Lamberti, C.; Prestipino, C.; Damin, A.; Bordiga, S.; Pelizzetti, E.; Zecchina, A. *J. Am. Chem. Soc.* **2003**, *125*, 2264.
(17) Goa, Y.; Yoshitake, H.; Wu, P.; Tatsumi, T. *Microporous Mesoporous Mater.* **2004**, *70*, 93.

Table 1. Postsynthesis Treatment Conditions of ETS-10 and the Quantity of Ti Removed from the Materials

sample	postsynthesis treatment conditions		Ti removed (wt %)
	H_2O_2 concentration (wt %)	contact time (min)	
	Single Treatment		
5/ETS-10	5	5	0.23
10/ETS-10	10	10	0.34
20/ETS-10	20	20	0.72
30/ETS-10	30	30	1.15
	Repeated Treatment with New Solution		
1×10/ETS-10	1×10	1×20	0.40
2×10/ETS-10	2×10	2×20	0.18
3×10/ETS-10	3×10	3×20	0.09

ments at 87 K using a Micromeritics ASAP 2010 analyzer. The samples were outgassed under vacuum at 573 K overnight. The free spaces of the sample tubes on top of the samples were determined volumetrically by helium manometry. To avoid helium entrapment in small micropores at 77 K, we allowed the samples to heat up again to 573 K for 1 h after the free-space measurements. The micropore volume was evaluated by the *t*-plot method.[18] As reference material for the t-plot analysis, nonporous titanosilicate was used that was obtained by calcining ETS-4 at 873 K. Pore size distributions in the micropore region were calculated from argon adsorption isotherms (87 K) using the nonlocal density functional theory (NLDFT) kernel contained in the Autosorb 1.51 software package provided by Quantachrome.[19] In N_2 (77K) and Ar (87K) adsorption experiments, 30 data points were precisely measured in the range of relative pressure between 1×10^{-6} to 1×10^{-1} to investigate the subtle changes in the microporosity of the materials. Raman spectra were measured at room temperature on a Nicolet Nexus FT-IR spectrometer with an excitation wavelength of 1064 nm (Nd:YAG laser). Diffuse reflectance IR Fourier transform (DRIFT) spectra were collected on a Nicolet Magna-IR 560 spectrometer. Samples were preheated at 573 K in a stream of N_2 gas for 2 h in an IR cell to achieve complete dehydration. ^{29}Si MAS NMR spectra were measured on a Bruker Avance 500WB NMR spectrometer using a 4 mm MAS probe. The single-pulse excitation spectra were measured with a recycle delay of 90 s (240 scans) and $\pi/4$ pulses of 2.2 μs at a spinning rate of 10 kHz. The cross-polarization spectra were obtained with proton $\pi/2$ pulses of 6 μs, a contact time of 4 ms, and a recycle delay of 5 s (8000 scans) at a spinning rate of 6 kHz. Because dehydration of ETS-10 has a significant effect on the width and position of the ^{29}Si MAS NMR lines,[20] the samples were allowed to equilibrate in a saturated water atmosphere at room temperature for 20 h prior to the measurements. Diffuse reflectance UV−vis spectra were recorded on a Varian Cary 5 spectrophotometer using $BaSO_4$ as reference. Transmission electron micrographs were obtained on a Hitachi 7500 transmission electron microscope operating with an acceleration voltage of 100 kV.

Results and Discussions

The X-ray diffraction patterns of the different ETS-10 samples (unmodified and modified) are shown in Figure 2.

The XRD patterns show that well-crystallized ETS-10 was investigated. Additional peaks belonging to other common titanosilicate impurities, such as ETS-4, AM-1, or AM-3,[21−23] were not observed. Only a minute impurity of α-quartz was identified (asterisks in Figure 2). Even after treatment with 30 wt % H_2O_2 concentration for a longer contact time, the resulting ETS-10 sample still exhibits a high crystallinity. The treated titanosilicate framework was also preserved after calcination at 773 K for 4 h (diffractograms not shown), indicating that the materials have a stability comparable to that of as-made ETS-10. Hydrogen peroxide treatment of ETS-10 results in the leaching of Ti atoms from its structure (Table 1) but not in a structure collapse.

A maximum amount of 1.15 wt % Ti was leached from the starting material after single treatment with 30 wt % H_2O_2 for 30 min. Repeating the treatment with fresh hydrogen peroxide solution seemed to be less efficient than using a higher hydrogen peroxide concentration. After removal of 0.40 wt % during the first treatment, only 0.09 wt % Ti was removed after the third treatment with fresh 10 wt % H_2O_2, which seems to indicate a passivation of the structure. The relatively low degree of leaching of Ti atoms from the ETS-10 structure seems to be advantageous for the preservation of the structure. In fact, there are no indications of significant changes of the crystallinity of any of the ETS-10 samples (see XRD).

The nitrogen physisorption isotherms of the samples are shown in Figure 3. The ETS-10 samples have type I isotherms according to the classification of Brunauer, Emmett, and Teller,[24] which is typical for microporous materials. The materials have specific external surface areas of 8 ± 1 $m^2\ g^{-1}$. At very low relative pressures in the range of 1×10^{-6} to 1×10^{-4}, a significant change of the adsorption behavior of the H_2O_2-treated ETS-10 is observed in comparison with that of the parent sample. The knees in the isotherms of the modified samples become flatter throughout the series (panels a and b of Figures 3). This effect is proportional to the H_2O_2 concentration and the time of exposure to H_2O_2 solution. The flattening of the isotherms is related to the presence of larger pores (supermicropores) in the crystals, which are formed during the H_2O_2 treatment. Such larger pores form as the result of a partial elimination of Ti atoms from the Ti−O−Ti chains and, most likely, the removal of SiO_x species that were previously linked to the TiO_6 octahedra. In addition, the micropore volume of the samples increased slightly after H_2O_2 treatment. This effect

(18) Cranston, R.; Inkley, F. *Adv. Catal.* **1957**, *9*, 143.
(19) Cracknell, R. F.; Gubbins, K. E.; Maddox, M.; Nicholson, D. *Acc. Chem. Res.* **1995**, *28*, 281.
(20) Zibrowius, B.; Weidenthaler, C.; Schmidt, W. *Phys. Chem. Chem. Phys.* **2003**, *5*, 773.
(21) Rocha, J.; Ferreira, A.; Lin, Z.; Anderson, M. W. *Microporous Mesoporous Mater.* **1998**, *23*, 235.
(22) Pavel, C. C.; Vuono, D.; Catanzaro, L.; De Luca, P.; Bilba, N.; Nastro, A.; Nagy, J. B. *Microporous Mesoporous Mater.* **2002**, *26*, 227.
(23) Lv, L.; Su, F.; Zhao, X. S. *Microporous Mesoporous Mater.* **2004**, *76*, 113.
(24) Brunauer, S.; Emmett, P. H.; Teller, E. J. *J. Am. Chem. Soc.* **1938**, *60*, 309.

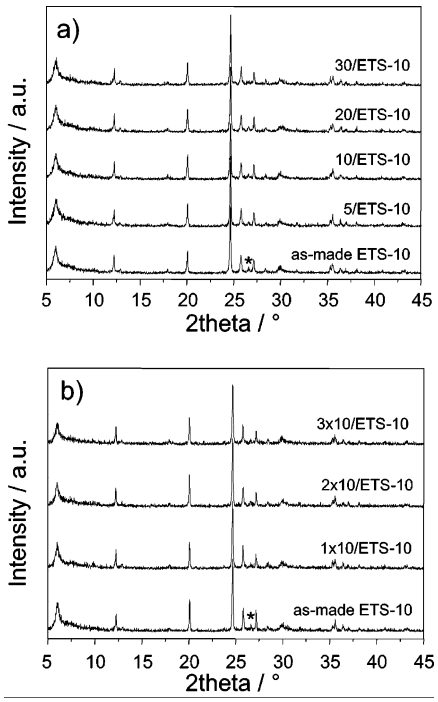

Figure 2. X-ray diffraction patterns of ETS-10 modified by (a) single H_2O_2 treatment and (b) repeated treatment with fresh solution. The asterisks denote peaks assigned to a very small amount of a quartz by-phase.

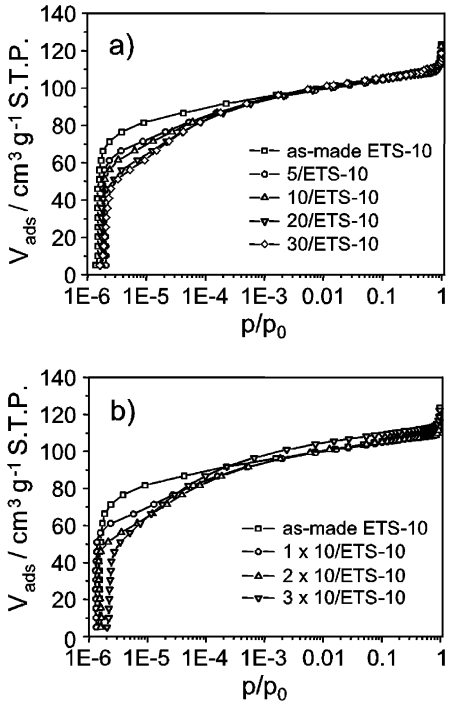

Figure 3. High-resolution N_2 adsorption isotherms of ETS-10 samples measured at 77 K after (a) a single H_2O_2 treatment and (b) repeated treatment with new solution (conditions for post-treatments given in Table 1).

is more pronounced after treatment under more severe conditions, as shown in Figure 4. A maximum micropore volume of 0.1645 cm^3/g was reached after three repeated treatments of ETS-10 with 10 wt % H_2O_2 for 20 min.

The micropore size distribution was determined by Ar adsorption experiments at 87 K. Argon was used to account for the presence of strong polar groups in the treated samples that could interact with N_2 because of its quadrupole momentum. The latter could result in enhanced interaction

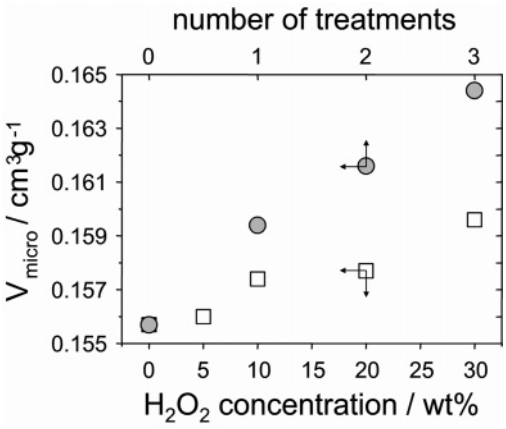

Figure 4. Evolution of the micropore volume in ETS-10 samples upon H_2O_2 treatment as determined by the *t*-plot method (the errors for the micropore volumes from the *t*-plot are in the range of 0.2−0.3% for the individual data points). Squares indicate micropore volumes of samples obtained by single treatments, circles those of samples obtained by repeated treatments according to Table 1.

with the polar sites of the titanosilicate framework, making it more difficult to discriminate between effects due to the variation of pore sizes and the presence of polar sites in ETS-10.[25] Furthermore, Ar adsorption in micropores occurs at higher p/p_0 values compared to N_2, making it more favorable for accurate investigations of micropores.[26] The Ar adsorption isotherms and the respective pore size distributions (PSD) determined by the NLDFT approach of as-made and modified ETS-10 samples are shown in Figure 5.

The pore size distribution of as-made ETS-10 shows a single maximum at about 0.72 nm. In contrast, the modified-ETS-10 samples have a bimodal micropore size distribution. The first type of pores has an effective size identical to that of the parent ETS-10, the second type corresponds to larger pores. The intensity of the second peak increases throughout the series. These observations can be explained by the formation of larger micropores (supermicropores) in ETS-10 during the postsynthesis treatment with H_2O_2.

Raman, DR UV−vis, IR, and TEM analyses of the modified ETS-10 samples were performed to examine the effect of the treatment conditions (H_2O_2 concentration and contact time) on the number and type of defects in the structure. Raman spectroscopy allowed us to study the local structure around the titanium atoms and thus was very useful for the investigation of the defects in ETS-10. The Raman spectra of the ETS-10 samples are shown in Figure 6.

The main band in the Raman spectrum of ETS-10 at ca. 724 cm^{-1} has been attributed to the Ti−O stretching mode of the Ti−O−Ti chains.[27−30] According to recent reports,[31,32]

(25) Groen, J. C.; Peffer, L. A. A.; Pérez-Ramírez, J. *Microporous Mesoporous Mater.* **2003**, *60*, 1.
(26) Ravikovitch, P. I.; Vishnyakov, A.; Russo, R.; Neimark, A. V. *Langmuir* **2000**, *16*, 2311.
(27) Mihailova, B.; Valtchev, V.; Mintova, S.; Konstantinov, L. *Zeolites* **1994**, *16*, 22.
(28) Ashtekar, S.; Prakash, A. M.; Kevan, L.; Gladden, L. F. *Chem. Commun.* **1998**, 91.
(29) Rocha, J.; Brandão, P.; Pedrosa de Jesus, J.; Philippou, A.; Anderson, M. W. *Chem. Commun.* **1999**, 471.
(30) Su, Y.; Balmer, M. L.; Bunker, B. C. *J. Phys. Chem. B* **2000**, *104*, 8160.
(31) Llabrés i Xamena, F. X.; Damin, A.; Bordiga, S.; Zecchina, A. *Chem. Commun.* **2003**, 1514.

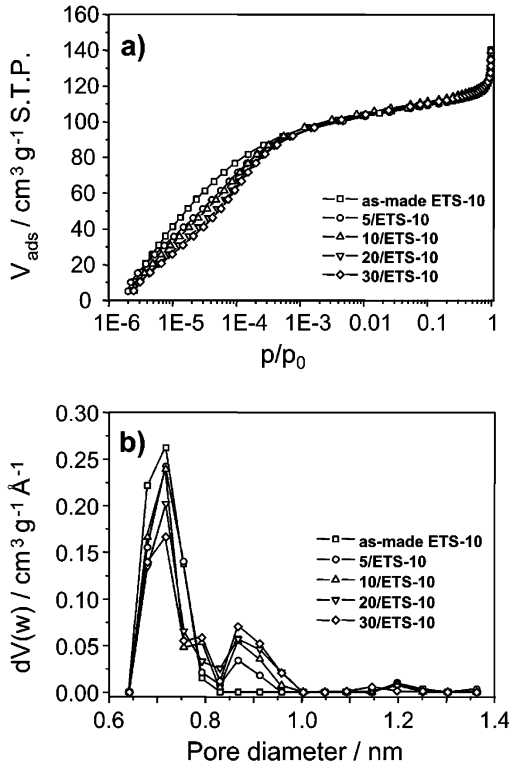

Figure 5. (a) High-resolution Ar adsorption isotherms and (b) NLDFT pore size distributions derived from the adsorption branches for ETS-10 as a function of the H_2O_2 concentration.

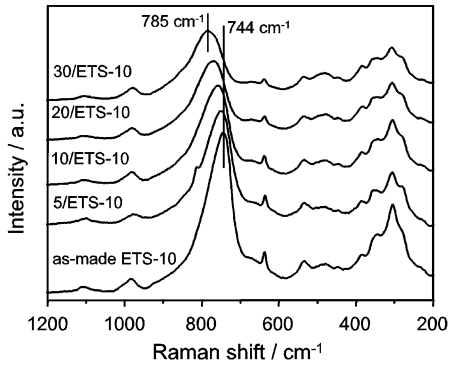

Figure 6. Raman spectra of the as-made and modified ETS-10 samples in the range 200−1200 cm^{-1}.

this band is mainly due to a totally symmetric combination of coupled Ti−O stretching modes in the chains of titania octahedra. The position and the breadths of this Raman band are suited as indicators for the concentration of defects in the sample and, consequently, of the average length of the Ti−O−Ti chains.[13,31] The Raman spectrum of our as-made ETS-10 shows a band at 744 cm^{-1}, which is already rather broad and shifted with respect to the band at about 724 cm^{-1} reported for nondefective ETS-10.[13,27−31] This indicates that our as-synthesized ETS-10 was already rather defective, which could be attributed to stacking defects formed during the crystallization process. The presence of stacking defects could in fact enhance the reactivity of disordered ETS-10 with hydrogen peroxide. The ETS-10 samples show an additional shift to higher frequencies (up to 41 cm^{-1} for the last sample) after H_2O_2 treatment and a progressive broadening with respect to the spectrum of the as-made material. These changes are associated with the induced defects in the ETS-10 samples, i.e., interruptions in Ti−O−Ti chains and shortening of the average $(Ti-O)_n$ chain length. Our results are qualitatively consistent with those of Southon and Howe.[13] They reported a stretching mode at about 724 cm^{-1} associated with titania chains that gets broadened and shifted with an increasing number of stacking defects in ETS-10. The effect is explained by coupling of Ti−O stretching modes in ETS-10 in analogy with the coupled C−C stretching vibrations of graphite as its crystal size is reduced.

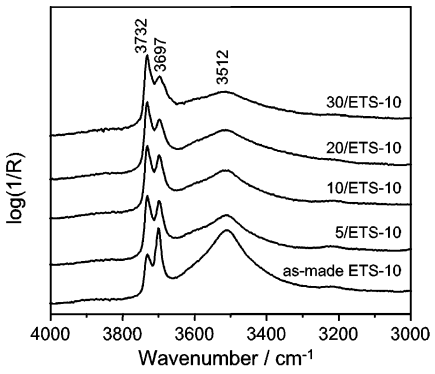

Figure 7. DRIFT spectra of the as-made and H_2O_2-treated ETS-10 samples evacuated at 573 K for 2 h in a stream of inert gas.

As a consequence of the disruption of Ti−O−Ti chains and partial leaching of Ti atoms, the formation of new hydroxyl groups is observed in DRIFT spectra of dehydrated samples (Figure 7).

The spectra all show two sharp dominant signals at 3732 and 3697 cm^{-1} and a broad band around 3300−3600 cm^{-1} that vary in intensity. There are only few reports on the assignment of IR bands in the O−H stretching region of ETS-10. Whereas the first two bands at around 3732 and 3697 cm^{-1} are most likely due to isolated Si−OH and Ti−OH groups, for example, on the external surface of the crystallites, the broad band with the maximum at 3512 cm^{-1} has been only tentatively assigned to H-bridged surface hydroxyl groups of both Si and Ti.[33,34] On the other hand, Southon and Howe have found additional bands at 3488 and 3200 cm^{-1} in FTIR spectra of ETS-10 outgassed under vacuum. They claimed that these bands correlate best with defect levels of ETS-10, suggesting that these signals could be associated with stacking faults.[13] In the spectra shown in Figure 7, only a weak signal at 3222 cm^{-1} was observed; it practically disappears completely after H_2O_2 treatment for a somewhat longer time. However, more interesting is the observed intensity inversion of the signals at 3732 and 3697 cm^{-1}, which is observed throughout the series. For the as-made ETS-10, the intensity of the band attributed to Ti−OH groups (3697 cm^{-1}) is bigger than that of the band assigned to the Si−OH groups (3732 cm^{-1}). Upon postsynthesis treatment, higher concentrations of H_2O_2 resulted in an increase in the number of Si−OH groups. Zecchina et al.

(32) Damin, A.; Llabrés i Xamena, F. X.; Lamberti, C.; Civalleri, B.; Zicovich-Wilson, C. M.; Zecchina, A. *J. Phys. Chem. B* **2004**, *108*, 1328.

(33) Robert, R.; Rajamohanan, P. R.; Hegde, S. G.; Chandwadkar, A. J.; Ratnasamy, P. *J. Catal.* **1995**, *155*, 345.

(34) Zecchina, A.; Llabrés i Xamena, F. X.; Pazè, C.; Turnes Palomino, G.; Bordiga, S.; Otero Areán, C. *Phys. Chem. Chem. Phys.* **2001**, *3*, 1228.

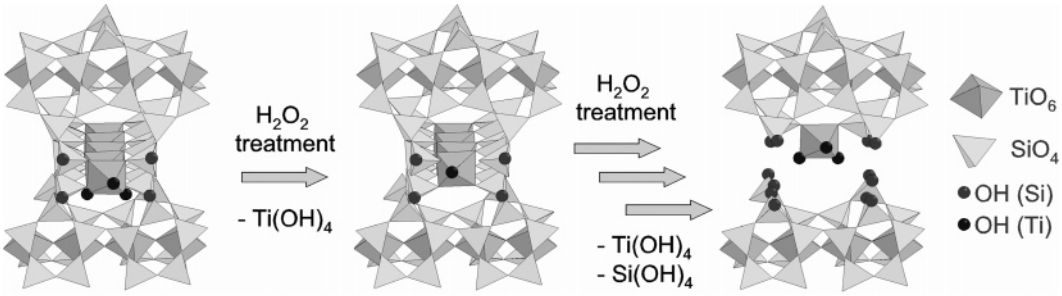

Figure 8. Formation of Si−OH groups after extraction of Ti from the ETS-10 structure.

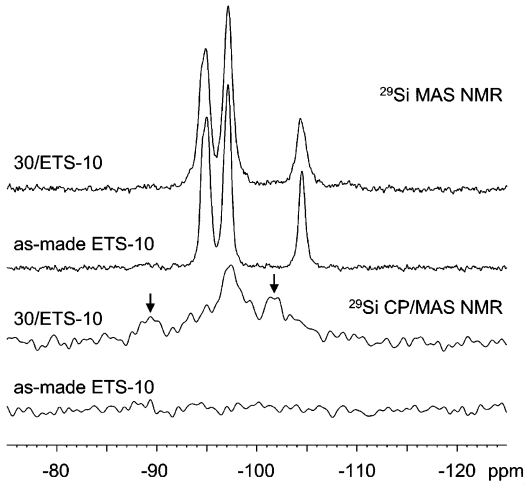

Figure 9. ^{29}Si MAS NMR spectra of as-made ETS-10 and 30/ETS-10 without and with cross polarization (CP). The two spectra on top were measured without and the two at the bottom with CP.

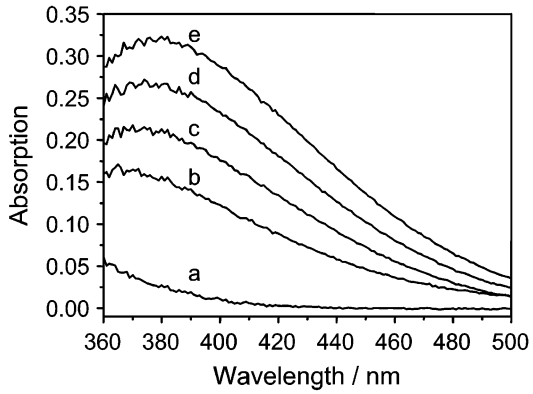

Figure 10. DR UV−vis spectra of (a) as-made ETS-10, (b) 5/ETS-10, (c) 10/ETS-10, (d) 20/ETS-10, and (e) 30/ETS-10 (for the assignment of the samples, see Table 1).

claimed that both silanol and titanol groups are located mainly at the external surface of crystallites but that they can also occur at internal structure defects.[34] The increase in the number of silanol groups in the modified ETS-10 sample may be tentatively explained as shown schematically in Figure 8.

Extraction of Ti from the ETS-10 structure during H_2O_2 treatment creates a large number of new silanol groups. Silica in the vicinity of the extracted Ti is also removed to a substantial extent. Upon removal of such Si species from the structure, even more silanol groups will form, because they are bound to further Si atoms via oxygen bridges. The most-available Ti atoms, which can interact with H_2O_2, are in principle those at the external surface of the crystallites but also those adjacent to the staking faults. If the leaching process of Ti atoms starts from the exterior and continues through the framework, larger channels are formed because of the extraction of both Ti and Si from the structure. Whereas the number of Ti−OH groups located at the titania chain ends remains more or less constant, the number of silanol groups increases. The more Ti that is extracted from the structure, the more Si−OH groups will form. This process explains the increase in the intensity of the IR signal at about 3732 cm^{-1} (Figure 7).

^{29}Si MAS NMR spectra of as-made and H_2O_2-treated samples are shown in Figure 9. The resonance lines of the as-made materials are somewhat broader than those of the as-made materials we investigated in a previous study,[20] indicating that the structure of the starting material used here was already slightly defective and/or distorted. This is in good accord with the results from the Raman investigations. However, treatment with H_2O_2 leads to a significant further broadening of the ^{29}Si NMR lines, as shown in Figure 9. The CP measurement of the H_2O_2-treated sample shows two broad signals of low intensity that are not present in the as-made material (see arrows in Figure 9). These two signals are attributed to silanol groups. An increase in the silanol concentration after the H_2O_2 treatment is the most likely explanation for the occurrence of these signals. This agrees well with the results from the IR investigations.

The interaction of hydrogen peroxide with molecular sieves containing Ti^{4+} metal cations in tetrahedral coordination, in particular TS-1, has been well investigated in the past decade.[35−37] After adsorption of H_2O_2, the color of titanium silicalites changes from white to yellow. A new band at 26 000 cm^{-1} (385 nm) related to the formation of complexes with peroxy groups bound to Ti^{4+} is typically observed. For this reason, Llabrés i Xamena et al.[16] have used H_2O_2 as probe molecule for the determination of exposed Ti centers in ETS-10 after acid treatment with HF. A similar observation was made in this study. The ETS-10 samples became yellow after contact with H_2O_2 with different intensities of the yellow color. This color also remained after washing with deionized water and drying at 323 K. DR UV−vis spectra confirmed the formation of a new ligand-to-metal charge-transfer (LMCT) band at ca. 385 nm after contact of ETS-10 with H_2O_2 of different concentrations (Figure 10). It corresponds to a charge transfer from the peroxide moiety

(35) Notari, B. *Adv. Catal.* **1996**, *41*, 253.
(36) Vayssilov, G. N. *Catal. Rev. − Sci. Eng.* **1997**, *39*, 209.
(37) Ratnasamy, P.; Srinivas, D.; Knözinger, H. *Adv. Catal.* **2004**, *48*, 1.

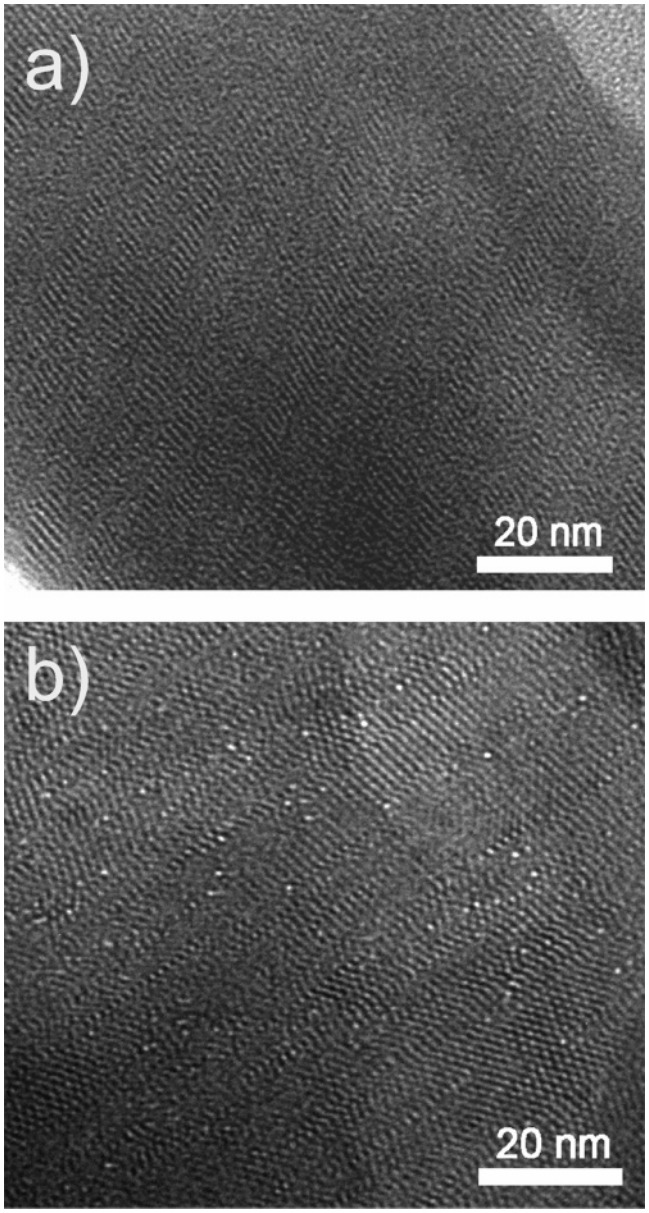

Figure 11. TEM micrographs of (a) as-made ETS-10 and (b) 30/ETS-10.

to the Ti center.[38] A progressive increase in the intensity of the band at 385 nm through the series is observed, suggesting the formation of an increasing number of Ti−O−OH groups. The Ti atoms available for the formation of such Ti−O−OH groups are those at the crystal surfaces and those at defects and interruptions of the titania chains.

During the postsynthesis treatment, H_2O_2 molecules can also interact with structural Ti atoms, leading to multiple breaks of the Ti−O−Ti chains and resulting in additional exposed titanium atoms. Therefore, the number of "active" Ti sites did progressively increase with increasing contact time and H_2O_2 concentration (Figure 10, spectra b−e).

TEM micrographs of as-made ETS-10 and 30/ETS-10 (treated with 30 wt % for 30 min) taken along the *a* or *b* direction, i.e., parallel to the layers of the two polymorphs, are shown in Figure 11. The large 12-membered rings pores of 0.48 × 0.76 nm, characteristic for the ETS-10 structure,

(38) Bordiga, S.; Damin, A.; Bonino, F.; Ricchiardi, G.; Lamberti, C.; Zecchina, A. *Angew. Chem., Int. Ed.* **2002**, *41*, 4734.

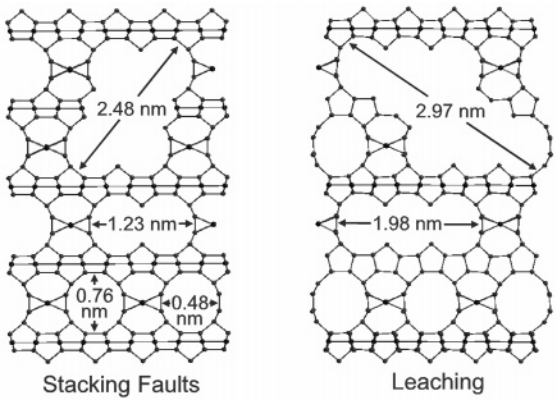

Figure 12. Structural representation of extended micropores in ETS-10 due to stacking faults (left) and leaching (right). Oxygen atoms connecting neighboring metal (Si, Ti) sites are omitted for simplicity. Probable pore dimensions were calculated from crystallographic data using the structure data reported by Wang and Jacobson.[4]

are identified by the bright spots. Changes in layer stacking sequences, represented by diagonal or zigzag and line defects, which normally appear in ETS-10 during crystallization, are also visible.

A significant number of larger white spots can be noticed in the TEM image of 30/ETS-10 that are not observed in the as-made sample. These spots are probably larger micropores (supermicropores) created after the extraction of Ti atoms together with the next-neighbor SiO_4 tetrahedra (= ($Ti^{[6]}$,$Si^{[4]}$)-spiro-5 units) from the structure. The resulting supermicropores presumably correspond to channels formed by rings containing 24 oxygen-bridged Si atoms (24-membered ring) with theoretical dimensions of ca. 0.76 × 1.98 nm (see Figure 12). The induced supermicropores are supposed to be larger than the double pore defects, resulting in 18-membered rings (0.76 × 1.23 nm), which was noticed by Anderson et al.[2] as the consequence of stacking faults. The creation of such larger supermicropores is supported by the bimodal micropore size distributions observed after H_2O_2 posttreatment and the enhancement of the micropore volumes.

Also, even larger pores may form by coalescence of pores from neighboring layers. Pores with diameters of about 2.48 nm could thus be formed if these pores are caused by stacking faults as reported by Anderson and coworkers.[3] However, much larger pores could be created by Ti extraction, as exemplified by the 2.97 nm pore shown in Figure 12.

Conclusions

Postsynthesis treatments with aqueous solutions of H_2O_2 (5−30 wt %) for different times induced structural defects in ETS-10 by partial removal of the structural Ti atoms without a substantial degradation in the crystallinity. The microporosity of H_2O_2-treated ETS-10 samples was significantly modified in comparison with that of the as-made material. The micropore volumes increased slightly after hydrogen peroxide treatment. The presence of a bimodal micropore size distribution in H_2O_2-treated ETS-10 samples was attributed to the creation of supermicropores resulting from the removal of ($Ti^{[6]}$,$Si^{[4]}$)-spiro-5 units from the

structure. These defective sites were already generated at relatively mild conditions (5 wt % H_2O_2 for 5 min). However, their number increased significantly with increasing H_2O_2 concentration and contact time. TEM micrographs of H_2O_2-treated ETS-10 revealed the presence of larger micropores (supermicropores). Partial removal of Ti atoms from the ETS-10 framework led to the interruption of titania chains and resulted in the formation of exposed Ti centers at the ends of the interrupted chains. The broadening and blue shift of the intense Raman band at 744 cm^{-1} proves the shortening of the average length of the titania chains. A substantial fraction of the accessible titanium sites that are formed during the treatment interacted with H_2O_2, resulting in the formation of Ti−O−OH groups. Treatment with H_2O_2 solution is thus a method that allows for the creation of larger micropores (supermicropores) in ETS-10 crystallites, making these materials interesting for fields in which transport limitations of molecules play an important role, e.g., for catalysis and gas separation.

Acknowledgment. We thank E. Löffler, University of Bochum, for Raman spectroscopic investigations and B. Zibrowius, MPI für Kohlenforschung, for NMR spectroscopic investigations and both of them for helpful discussions. Furthermore, we thank the Deutsche Forschungsgemeinschaft (Schm 936/4-1) and the Max Planck Gesellschaft for financial support.

CM052261J